

Correction of the temperature effect in calibration of a solar radio telescope

Li-Hong Geng¹, Cheng-Ming Tan^{1,2}, Yi-Hua Yan^{1,2}, Bao-Lin Tan^{1,2}, Dong-Hao Liu¹ and Jin-Ping Dun³

¹ CAS key Laboratory of Solar Activity, National Astronomical Observatories of Chinese Academy of Sciences, Beijing 100101, China; genglh@nao.cas.cn

² School of Astronomy and Space Sciences, University of Chinese Academy of Sciences, Beijing 100049, China

³ Key Laboratory of Space Weather, National Center for Space Weather, China Meteorological Administration, Beijing 100081, China

Received 2020 October 29; accepted 2021 January 25

Abstract This work analyzes the annual fluctuation of the observation data of the Mingantu Solar radio Telescope (MST) in S, C and X bands. It is found that the data vary with local air temperature as the logarithmic attenuation of equipment increases with temperature and frequency. A simplified and effective calibration method is proposed, which is used to calibrate the MST data in 2018–2020, while the correction coefficients are calculated from data in 2018–2019. For S, C and X bands, the root mean square errors of one polarization are 2.7, 5.7 and 20 sfu, and the relative errors are 4%, 6% and 8% respectively. The calibration of MUSER and SBRS spectra is also performed. The relative errors of MUSER at 1700 MHz, SBRS at 2800 MHz, 3050 MHz and 3350 MHz are 8%, 8%, 11% and 10% respectively. We found that several factors may affect the calibration accuracy, especially at X-band. The method is expected to work for other radio telescopes with similar design.

Key words: instrumentation — polarimeters methods — data analysis — methods: observational

1 INTRODUCTION

A solar radio telescope plays an important role in observing and revealing the physical processes of the solar atmosphere, solar flares, coronal mass ejections and other solar activities. It is one of the most important means to monitor and study the solar-terrestrial space weather. Solar radio radiation flux is related to the sunspot number, white light flare, X-ray flare and energetic particle event, among which the 10.7cm flux is an important indicator of such solar activities (Liu et al. 2010; Wen et al. 2010; Klein et al. 2018; Schonfeld et al. 2015). Currently, solar radio telescopes are operating world-widely, such as Phoenix (100–4000 MHz; Benz et al. 1991), Ondrejov spectrometer (800–5000 MHz; Jiricka et al. 1993), the Solar Broadband Radio Spectrometer (SBRS) (Fu et al. 1995; Fu et al. 2004; Ji et al. 2005) and the Mingantu Spectral Radiograph (MUSER) etc. (Yan et al. 2009).

Calibration is a crucial step to obtain more reliable results from observation. For multi-dish telescopes such as MUSER, single-dish calibration is fundamental. In the early times, absolute calibration was used. The antenna gain was extracted from radar and communication

technology while its sensitivity was obtained through experiments.

At present, because of the difficulty in obtaining the absolute calibration value, the method is usually only applicable to radiometers with single frequency (Brotten & Medd 1960; Findlay 1966; Tanaka et al. 1973). Messmer et al. (1999) developed a relative calibration method, which refers to the standard source to calculate the radiation (or brightness temperature). This method is usually used in spectrum analyzer, because the absolute calibration of spectrometer is a complex task in broadband frequency. Yan et al. (2002) found that nonlinear effect during strong solar radio bursts can have a significant effect while Tan et al. (2009, 2015) found that the calibration coefficient of SBRS varied with the local air temperature, and therefore temperature wavelet correction calibration methods were proposed, which resulted in an improvement of calibration result comparing to that of constant coefficient calibration.

In this work, the observation data of the Mingantu Solar radio Telescope (MST) (Geng et al. 2018) in Mingantu Observing Station (42.22°N, 115.24°E) is analyzed, and an improved temperature correction calibration

method is discussed. Since January 2018, MST flux data appears annual fluctuation ranging about 2 dB, 2 dB and 3 dB in S, C and X bands, which are corresponding to 2801, 4542 and 9084 MHz, as shown in Figure 1.

Through detailed examination of various influencing factors including system design, variation of distance between the Sun and the Earth, air temperature and sky background, the local air temperature is found to be most responsible for the fluctuation: MST system gain varies with air temperature and frequency. From data in the year of 2018–2019 of local air temperature, standard flux and MST, six sets of temperature correction coefficients are obtained. By applying these coefficients to MST data in the year of 2018–2020, the residual mean square deviation of single polarization reduces to 2.7 sfu, 5.7 sfu and 20 sfu, with relative errors of about 4%, 6% and 8%, respectively. A similar method has been applied to the calibration of SBRS at 2800/3050/3350 MHz in 2.6–3.8 GHz frequency range and MUSER on 1700 MHz with relative errors of 8%, 11%, 10% and 8% respectively.

2 METHOD

2.1 Relative Calibration Method and Standard Flux

Lu L. et al. calibrated the 4.5 GHz–7.5 GHz Solar Radio Spectrometer of the Purple Mountain Observatory using NoRP (the Nobeyama radio polarimeters) data at 3.75 and 9.40 GHz as standard flux. The method to determine the calibration constant is shown in Equation (1).

$$C_A(f) = \frac{F_{qs}(f) \times (R_n(f) - R_t(f))}{(R_{qs}(f) - R_b(f))}, \quad (1)$$

where C_A is the calibration constant, F_{qs} is the standard source flux, R_n , R_t , R_{qs} and R_b are the observed values of noise source, matching terminal, the Sun and the sky background under the specific frequency channel. Calibration data were obtained at least once a day. Otherwise, it is the statistical average value of calibration constants across the past years, so as to reduce the dependence of other stations on standard sources. The relative standard deviation was within 10% in most channels. The temperature effect is not considered here.

Using relative calibration in conjunction with linear interpolation, Tan C.M. et al. conducted a systematic study on the calibration coefficients of SBRS (1.0–2.0 GHz, 2.6–3.8 GHz, 5.2–7.6 GHz) from 1997 to 2007 with NGDC data as standard flux data. It was found that the instrument is affected by the local air temperature. Thus the calibration coefficient should include this factor as follows.

$$C_d(t) = C_1 + C_2 \times T_{\text{air}}(t), \quad (2)$$

where t is the date series of the year, $C_d(t)$ is the daily calibration coefficient, obtained from the average value or

Gaussian fitting value of the daily calibration coefficient in the past ten years for each frequency channel. Thus, 366 groups of C_1 and C_2 are obtained by a least square method.

Wang L. et al. calibrated Mengcheng Solar Radio Spectrometer (McSRS, 12–16 GHz) and found that the results of traditional calibration methods were not ideal due to instrument electronics issues. It was improved by analyzing the relevant radiation mechanisms with the observation data of NoRP, NoRH and GOES assuming that the calibration coefficient varies with time linearly in the range of interest:

$$R_{\text{obs}} = F_{\text{obs}} \times (k \times t + b) + R_b, \quad (3)$$

where R_b , k and b are the parameters to be determined, t is time series, F_{obs} is standard flux, R_{obs} is the observed data.

When calibrating MST data, the atmosphere absorption and emission are neglected, because the local Earth atmosphere does affect the solar radio intensity, but it is usually neglected at a frequency lower than 17 GHz (Tsuchiya & Nagame 1965; Matsuura & Kaufmann 1968). Emissions from the Earth atmosphere are also neglected (Gurnett 1974, 1975), for the emission frequency being far away from MST frequency range.

Tsuchiya & Nagame (1965) pointed out that the solar radio wave suffers the Earth atmospheric absorption, and the absorption depends mostly on zenith distance and density of water vapor, while neglecting the effects of temperature and atmospheric pressure to the absorption. They concluded that the absorption of the terrestrial atmosphere does not affect the flux measurement of the 17 GHz radio polarimeter at the Tokyo Astronomical Observatory. In solar radio astronomy tropospheric absorption effects are usually neglected at wavelengths larger than 3 cm (10 GHz), but important errors can result when flux measurements are performed at larger zenithal angles (low Sun elevation), even in the centimeter-decimeter wavelength range (Matsuura & Kaufmann 1968).

Tan et al. (2015) discussed that the Sun elevation have a small effect on the SBRS calibration because the calibration performed around noon with high Sun elevation. Furthermore, they emphasized that according to the analysis of atmosphere absorption, the solar flux should be larger in summer (high elevation) than that in winter (low elevation). However, the situation of the MST observation is on the opposite: the observed data is higher in winter and lower in summer, as shown in Figure 1.

Gurnett (1974) and Gurnett (1975) had done some research on the Earth as radio source. They presented that the Earth emits very intense electromagnetic radiation in the frequency range 50–500 kHz, and the Earth also radiates a weak non-thermal continuum radiation

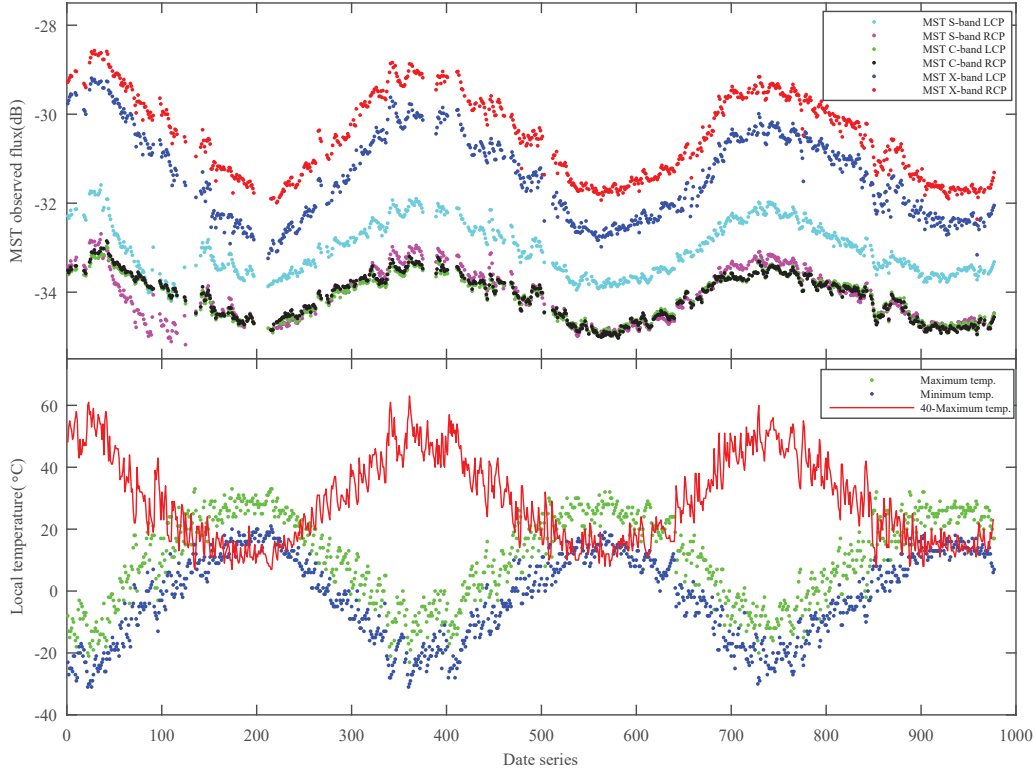


Fig. 1 (Top) MST observed raw data of solar radio flux in S/C/X bands of left and right circular polarization channels in 2018 Jan. 1–2020 Aug. 31; (Bottom) Local everyday maximum, minimum and difference temperature (40°C- maximum temperature) at the same time in Zhengxiangbaiqi, Inner Mongolia.

decreases with increased frequency and is usually below the cosmic noise level at frequencies above 100 kHz.

When calibrating MST data, the Sun-Earth distance compensation factor (peak to peak value 0.3 dB) is not large enough to explain MST data annual fluctuation (peak to peak value 2–3 dB). While the attenuation in logarithmic unit changing with ambient temperature of a 15 meter long low-loss coaxial cable explains the fluctuation. The cable is used to transmit solar signal from the radio front-end near the antenna-feed to the monitoring room where the MST indoor receiving system locates in. Relative calibration method with all parameters except the temperature in logarithmic unit is used to obtain the correction coefficient from standard flux and local air temperature:

$$A(N, f, P) = (R_{\text{obs}}(N, f, P) - F_{\text{ss}}(N, f, P)) / \Delta T(N), \quad (4)$$

where $A(N, f, P)$ is the temperature correction coefficient, $R_{\text{obs}}(N, f, P)$ is the daily observation value at 6:30 UT, $F_{\text{ss}}(N, f, P)$ is the standard solar radio flux. N, f, P are the date series of the year, the frequency and the polarization, respectively. $\Delta T(N)$ is the temperature difference of the day. It is the front-end box temperature of 40°C minus the maximum temperature of the day. The maximum and minimum temperature in the history of Zhengxiangbaiqi is in the range $\pm 37^\circ\text{C}$. It is conveniently

for the MST thermal-controlled front-end box to heat and keep its internal temperature stable in 40°C. As a result, the gain loss of electronic components in the front-end box will be usually smaller in 40°C ambient temperature than that in higher temperature. The MST data is a relative value, it increases with temperature decrease. So we use 40°C as the reference temperature, and 40-T(°C) as the temperature parameter.

Figure 2 shows the everyday $A(N, f, P)$ from Equation (4) of MST S, C and X band left and right polarization channels in 2018–2019. However, $A(f, P)$ is found to grow in inverse proportion to the temperature difference ΔT , as shown in Figure 3. Thus, six groups of the coefficient of $C_0(f, P)$ and $C_1(f, P)$ can be obtained by fitting the curve of $A(f, P)$ with ΔT , see Equation (5) and Table 1. The curves are also drawn in Figure 3. The corrected daily solar radio radiation flux $F_{\text{sun}}(N, f, P)$ can be calculated from Equation (6).

$$A(f, P, \Delta T) = C_0(f, P) + C_1(f, P) / \Delta T. \quad (5)$$

$$\begin{aligned} F_{\text{sun}}(N, f, P) &= R_{\text{obs}}(N, f, P) - A(f, P) \times \Delta T(N) \\ &= R_{\text{obs}}(N, f, P) - C_0(f, P) \times \Delta T(N) \\ &\quad - C_1(f, P). \end{aligned} \quad (6)$$

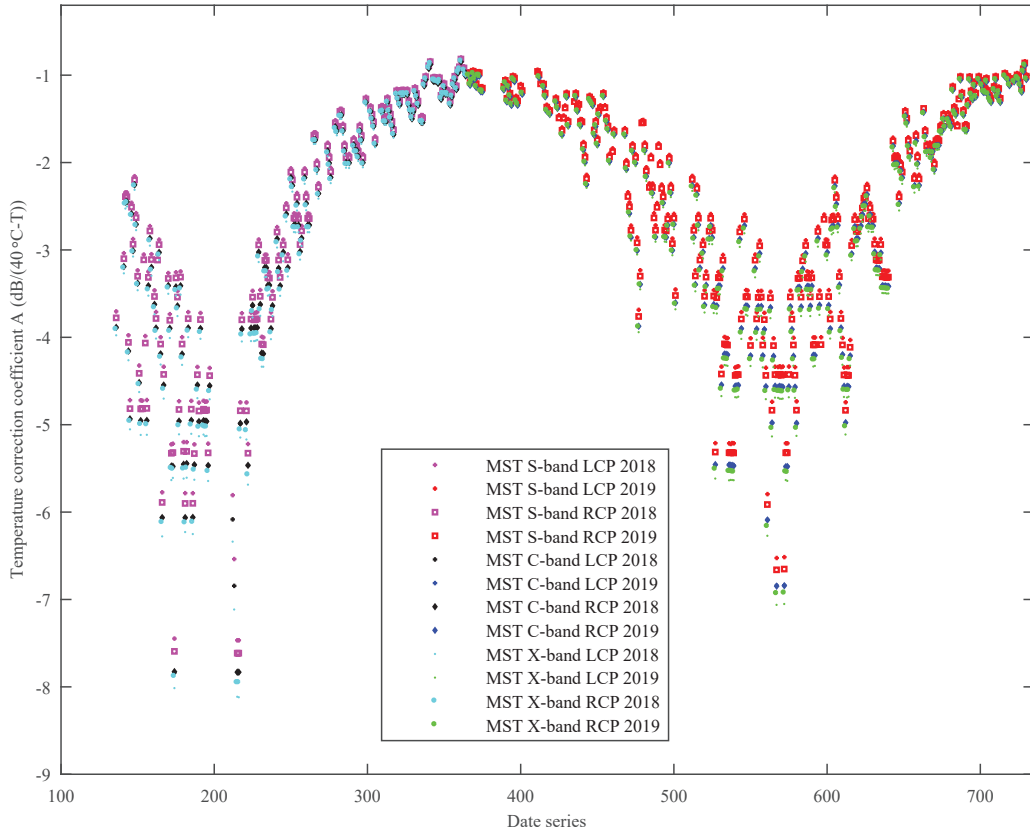


Fig. 2 The everyday correction coefficient $A(N, f, P)$ from Eq. (4) of MST S/C/X bands of Left and Right circular polarization channels in 2018–2019. X axis: date series from 20180101 to 20191231; Y axis: temperature correction coefficient (dB/°C).

Table 1 Fit Coefficient for MST S/C/X Bands of Left and Right Circular Polarization Channels in 2018–2019

Coefficient	SL	SR	CL	CR	XL	XR
	S-band LCP	S-band RCP	C-band LCP	C-band RCP	X-band LCP	X-band RCP
C_0	0.03696	0.03685	0.02631	0.02798	0.05465	0.05067
C_1	-52.50	-53.56	-54.94	-54.95	-56.94	-55.88

Table 2 RMSE and Mean Values of MST S/C/X Bands in Left and Right Circular Polarization Channels after Correction of Temperature Effect

Correction Error	SL	SR	S Total	Δ %	CL	CR	C Total	Δ %	XL	XR	X Total	Δ %
2018R	2.18	2.18	2.18	3.1	3.31	3.59	3.48	3.5	23.97	17.87	17.71	7.1
2018M	0.33	0.53	0.44	/	0.56	1.38	0.98	/	-1.79	3.79	1.60	/
2019R	2.32	2.33	2.31	3.3	3.68	4.06	3.82	3.8	20.92	19.44	19.93	8.0
2019M	-0.20	-0.12	-0.16	/	-0.29	-1.04	-0.66	/	1.54	0.63	1.08	/
2020R	2.50	2.91	2.65	/	5.03	5.65	5.26	5.3	20.30	19.81	19.71	7.9
2020M	-0.75	-1.37	-1.06	3.8	-1.91	-3.58	-2.74	/	3.04	-3.52	-0.25	/

2.2 MST Data Correction

Equation (6) and $C_0(f, P)$, $C_1(f, P)$ in Table 1 are applied to correct the annual fluctuation of MST observational data until 20200831. The root mean square errors at three bands are given by comparing the MST data after the temperature

correction with the standard flux. We use the variation of the peak-peak value of the annual fluctuation of MST data before and after correction (decreasing about 1.5 dB) to present the temperature correction effect. Figures 4 and 5 present the comparison between the corrected flux data and the standard flux data since 2018. Table 2 lists the

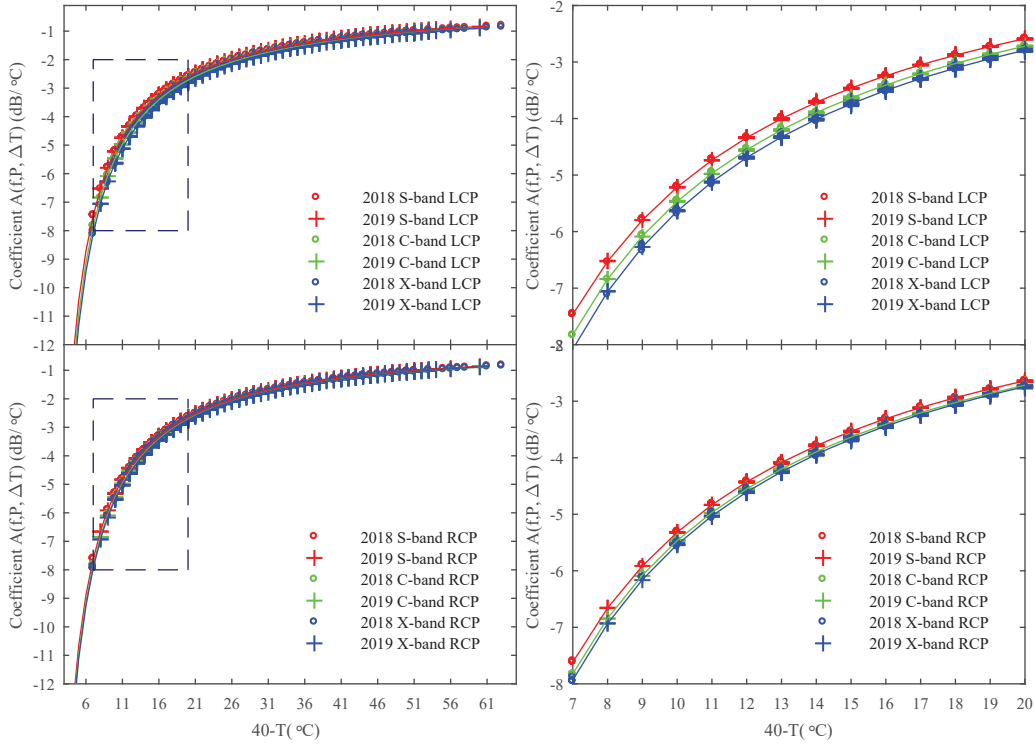


Fig. 3 Temperature correction coefficient $A(f, P, \Delta T)$ ($^{\circ}\text{C}$) of MST S/C/X bands in the left and right circular polarization channels vary with temperature difference $\Delta T = 40 - T_{\text{max}}$ ($^{\circ}\text{C}$) in 2018–2019. X axis: $\Delta T = 40 - T_{\text{max}}$ ($^{\circ}\text{C}$); Y axis: correction coefficient ($\text{dB}/^{\circ}\text{C}$).

Table 3 Left and Right Polarization Channels Correction Error of SBRS on 2800/3050/3350MHz, and MUSER on 1700MHz

Correction Error	Left Polarization sfu	Right Polarization sfu	Total Power sfu	Δ %
2800MHz/SBRS	3.97	3.72	7.54	0.08
3050MHz/SBRS	5.19	5.84	10.88	0.11
3350MHz/SBRS	4.56	5.19	9.44	0.10
1700MHz/MUSER	2.62	2.63	5.25	0.08

root mean square and mean value of residual error after correction in each year.

In Table 2, letters R and M follow the year 2018, 2019 and 2020 in the first column represent the RMSE (Root Mean Squared Error) and mean values separately for each year. Letters SL, SR, CL, CR, XL and XR in the first row represent the left and right polarization channel in S, C and X bands. S total means all observation data in both polarization channels in S band are used to obtain RMSE and mean values. So do the C total and X total. Symbol Δ represents the relative error and equals RMSE divided by average value of standard flux. For the year 2018–2020, Δ is estimated to be smaller than 4%, 6% and 8% in S, C and X bands with the average value of standard flux being about 70, 100 and 250 sfu.

The atmospheric absorption, severe temperature changes and standard flux fluctuation limit the accuracy

of temperature effect correction of the relative calibration method. After the correction, the flux in X-band still remains an annual change trend, as shown in Figures 4 and 5. Figure 6 summarizes the everyday maximum and minimum temperature of Zhengxiangbaiqi from 2014 to 2020. It can be seen that the temperature is relatively stable from June to September from year to year, while the temperature changes sharply in other times. But it is the rainy season in Zhengxiangbaiqi from June to September. In cloudy, rainy or snowy days, the atmosphere on Earth absorbs more radiation from the Sun especially that in X band for MST. In Figure 4, the low value deviated greatly from standards emphasized in the black ellipse are not caused by the solar activity, but the mild snowy weather on 2020 February 13–15 in Zhengxiangbaiqi. On the other way, NoRP flux data as standard also have obvious annual fluctuation at 3.75, 9.4 and 17 GHz, in Figure 7. The annual

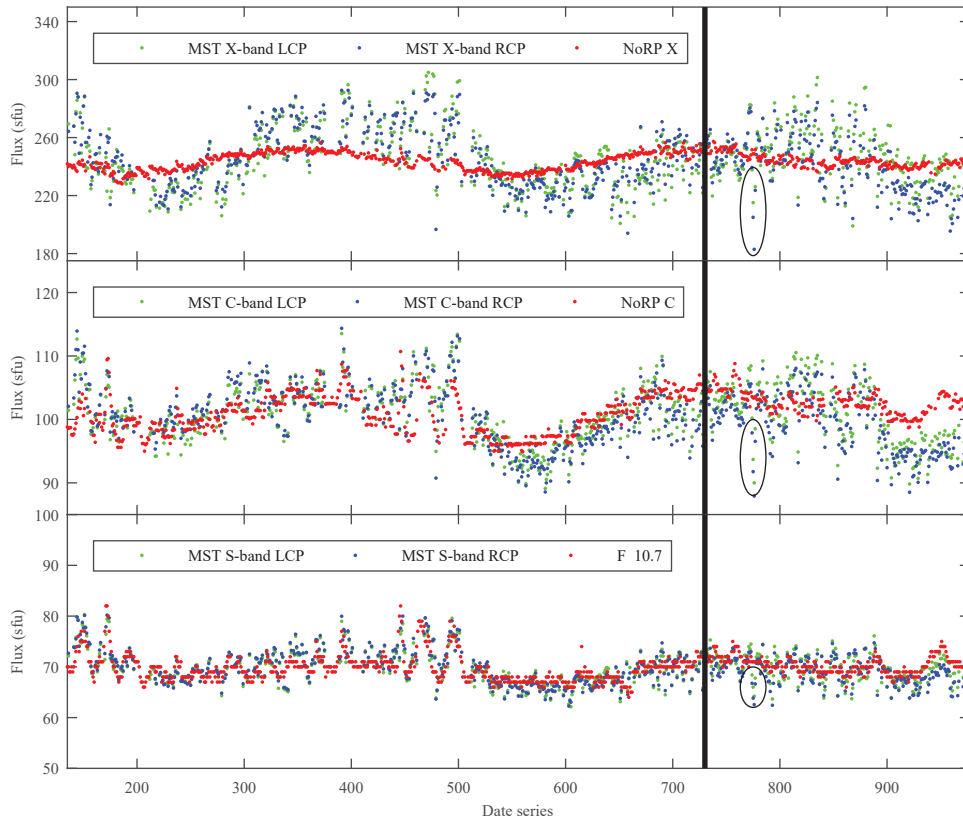


Fig. 4 MST temperature corrected solar radio flux (sfu) in 20180101–20200831 compared with standard flux of NoRP and F10.7. Three panels from bottom to top present the flux in S, C and X bands. The *black thick line* indicates separation of the year 2020 and 2019. MST observed data in 2020 are corrected by the coefficients obtained from data in 2018–2019. The low values in three ellipses are corresponding to continuous heavy snowy and cloudy days in Zhengxiangbaiqi on 2020 Feb. 13 to 15.

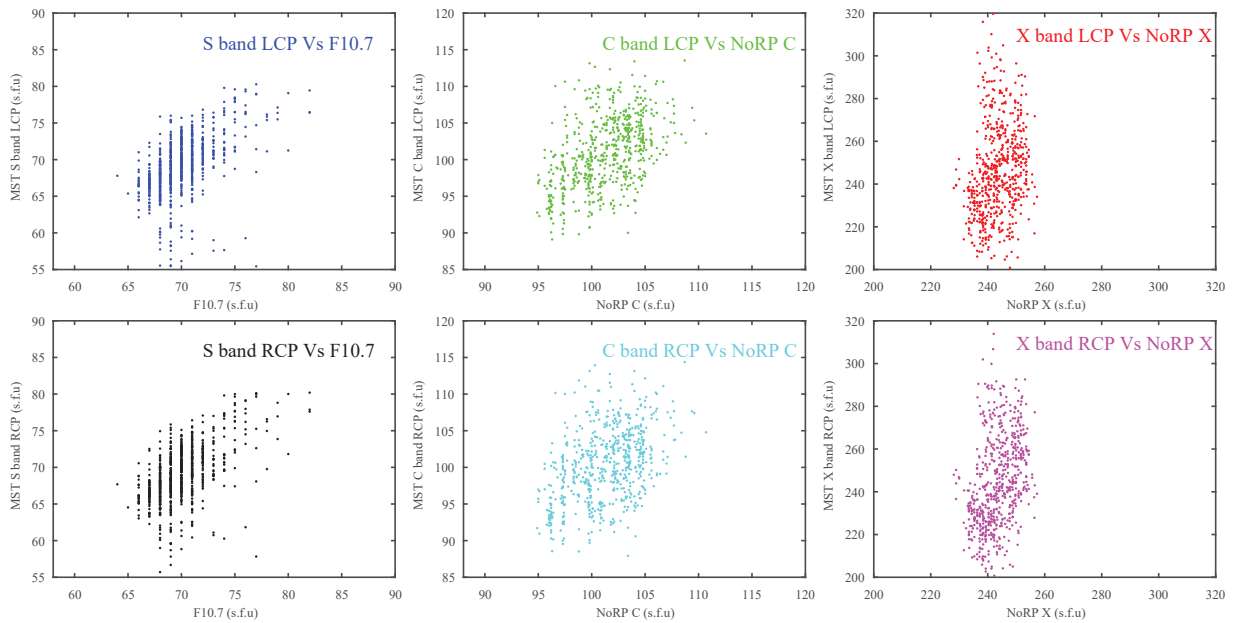


Fig. 5 MST temperature corrected solar radio flux (sfu) in 20180101–20200831 compared with standard flux of NoRP and F10.7. The three columns from left to right present the comparison in S/C/ X bands, the two rows from top to bottom present the comparison in LCP and RCP channels.

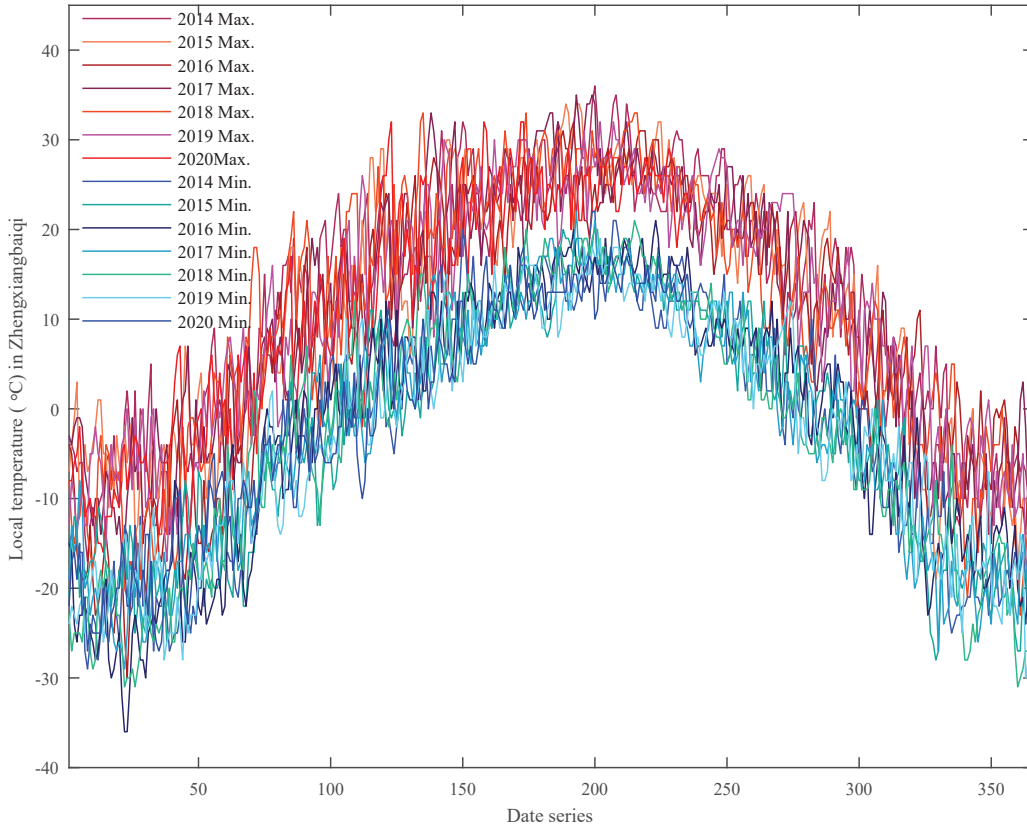


Fig. 6 Maximum and minimum local temperature in Zhengxiangbaiqi in 20140101–20200831. The range of temperature is +36°C to –36°C, and the maximum day temperature difference is 24°C.

variation range on 9.084 GHz obtained by interpolation is about 20 sfu. and that on 17 GHz is about 40 sfu.

In fact, the transmission loss of the 15m long coaxial cable had ever been measured in 10 ambient temperatures from –40°C to +60°C at five frequencies (2 GHz, 2.8 GHz, 4.5 GHz, 9.1 GHz and 10 GHz) before it was used on MST, showing that the cable had similar but not exactly the same temperature and frequency characteristics. This measurement was done by the 16th Research Institute of China Electronics Technology Group Corporation (CETC). When we realized that gain change of the long coaxial cable with the ambient temperature may cause the annual fluctuation of MST observation data, we asked the engineer in the 16th institute, CETC, if they had done some temperature experiments on the coaxial cable, they provided us a group data of the measurement. Figure 8 is plotted based on this measurement result. The temperature and frequency characteristics difference between the cable and MST is because MST receiving system is composed by more temperature sensitive electronic units than the cable, and there is a temperature gradient along the 15m long cable.

3 APPLICATION TO SBRS AND MUSER

The above-mentioned temperature correction method is applied to MUSER at 1700MHz and to the 2.6–3.8 GHz frequency band of the Huairou spectrum analyzer SBRS. Three frequency points 2800/3050/3350 MHz are selected from the 2001–2002 observation data and historical temperature. The left and right circular polarization temperature correction coefficients are obtained to correct the observation data in 2003. However, the sky background is considered, and the noise source and load are introduced to correct the R_{obs} . R_{obs} in Equations (4) and Equation (6) is replaced by formula (7). Equations (4) and (6) become Equations (8) and (9). Results applied to SBRS and MUSER is presented in Figures 9, 10, 11 and Table 3.

$$\frac{R_{\text{sun}}(N) - R_{\text{sky}}(N)}{R_n(N) - R_t(N)}. \quad (7)$$

$$A_1(N) = \left(\frac{R_{\text{sun}}(N) - R_{\text{sky}}(N)}{R_n(N) - R_t(N)} - F_{\text{sun standard}}(N) \right) / \Delta T(N). \quad (8)$$

$$F_{\text{sun}}(N) = (R_{\text{sun}}(N) - R_{\text{sky}}(N)) / (R_n(N) - R_t(N)) - C_0 \times \Delta T(N) - C_1. \quad (9)$$

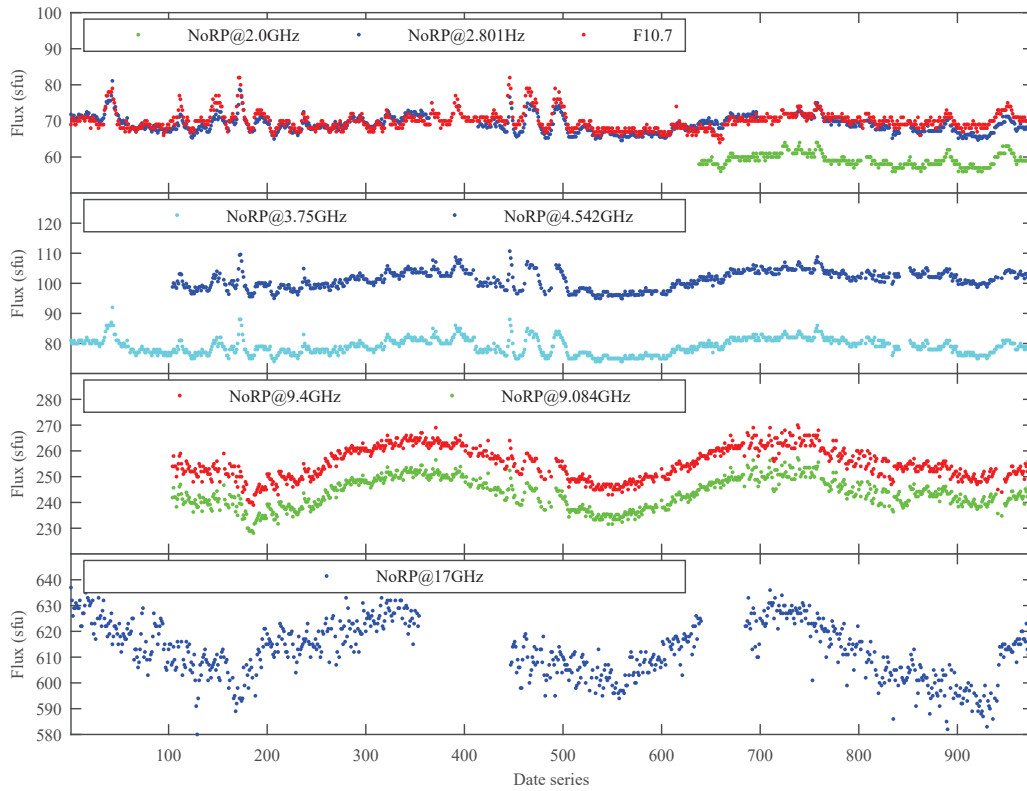


Fig. 7 Annual fluctuation of NoRP flux data. From top to bottom: NoRP 2.0 GHz, NoRP 2.801 GHz and F10.7; NoRP 3.75 GHz, NoRP 4.542 GHz; NoRP 9.4 GHz, NoRP 9.084 GHz; NoRP 17 GHz.

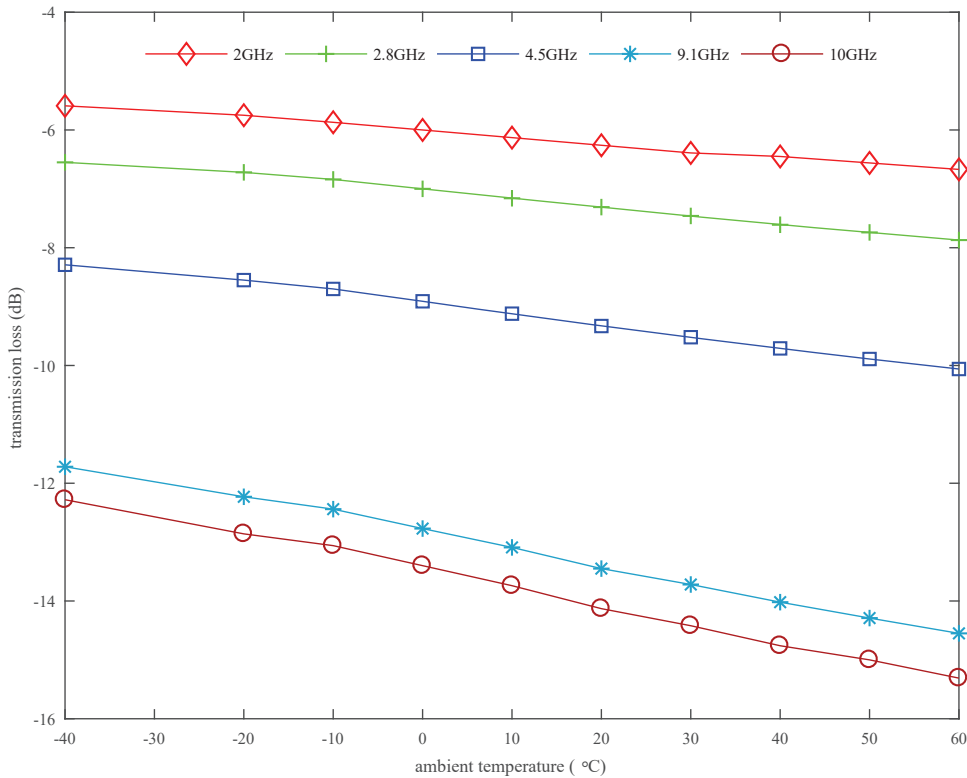


Fig. 8 The transmission loss of the 15 m long coaxial cable measured in 10 ambient temperatures from -40°C to $+60^{\circ}\text{C}$ at five frequencies (2 GHz, 2.8 GHz, 4.5 GHz, 9.1 GHz and 10 GHz) by 16th institute, CETC.

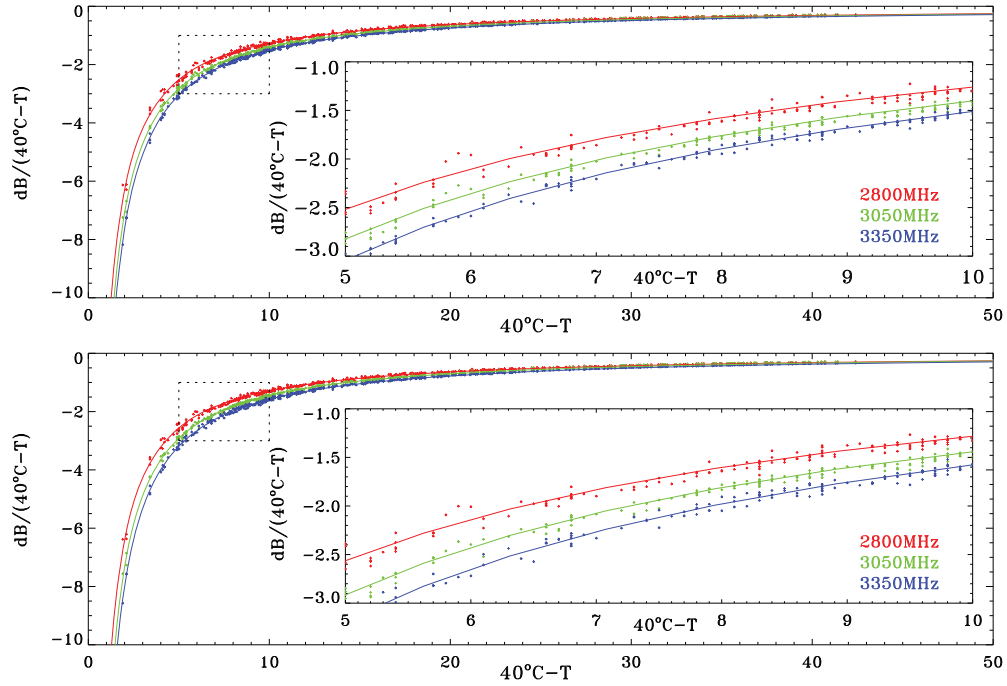


Fig. 9 SBRS 2800/3050/3350MHz left and right circular polarization correction coefficients vary with temperature difference from 42°C in 2001–2002. *X axis*: 42-the day’s maximum temperature (°C); *Y axis*: A1 (dB/°C).

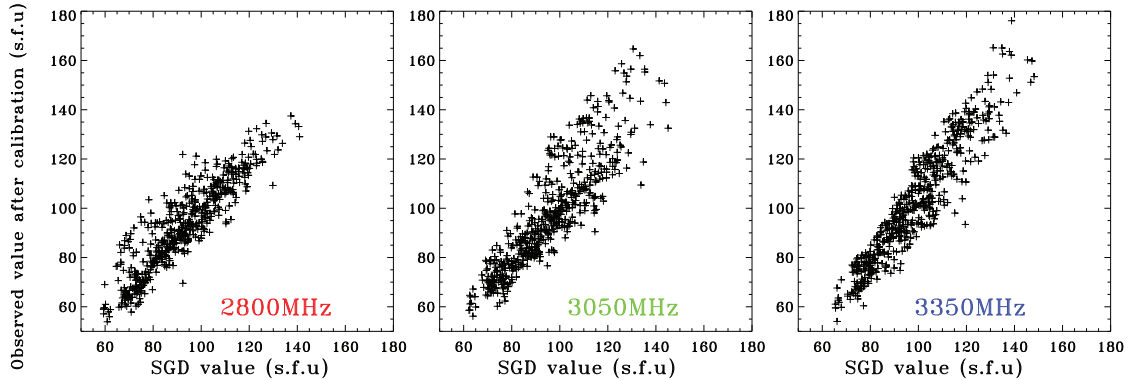


Fig. 10 Observed data after correction of SBRS on 2800/3050/3350MHz compared with standard data in 2003. *X axis*: standard values (sfu), *Y axis*: corrected values (sfu).

4 CONCLUSIONS

The annual fluctuation of MST observation data is mainly caused by long coaxial cable’s gain change with the ambient temperature. The relative calibration method proposed in this paper improves the temperature effect of MST, SBRS and MUSER observation data. However, there are several factors limit the calibration accuracy, especially for that in X-band of short wavelength. From the temperature correction results (Fig. 4, Fig. 5 and Table 2), the X band temperature correction effect is not ideal. So, firstly, the atmospheric absorption effect in short wavelength especially concerning the snowy, rainy and cloudy days may need to be considered in calibrating

telescope similar with MST. The grassland climate is rapidly changeable, which is a test for high-precision correction. Secondly, the annual fluctuation of standard flux data (Fig. 7) needs to be corrected before being used as standard source for MST. Thirdly, we use the maximum temperature (Fig. 6) in the day to correct the MST data on 6:30 UT. There is an error between maximum temperature and the real temperature. Finally, to avoid the temperature effect on radio telescope observation data, it is better to keep sensitive electronic equipment in a thermally controlled environment or replace it with low temperature sensitivity equipment. For example, using fiber cables and some optical-electronic transformer equipment to replace the long coaxial cable. This work provides a reference

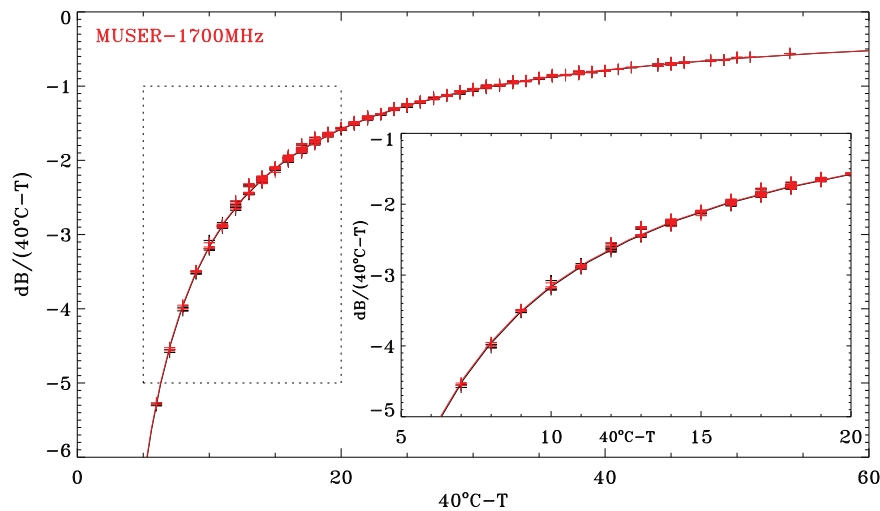


Fig. 11 MUSER 1700MHz left (black) and right (red) circular polarization correction coefficients vary with temperature difference from 42°C in 2015–2018.

for the design, observation operation, data processing and calibration of similar radio telescopes.

Acknowledgements This work is supported by NSFC (Grant Nos. 11433006, 11661161015, 11790301, 11790305, 11973057, 11773043, 11941003 and 2018YFA0404602), and the MOST grant (2014FY120300). In this paper, C and X bands standard solar flux are obtained by double logarithmic linear interpolation from NoRP (the Nobeyama Radio Polarimeter) published scientifically validated observational data from the website of Japan's Nobeyama Observatory (<http://solar.nro.nao.ac.jp/norp/data/daily>). S band standard solar flux uses the 10.7 cm data on the website of the National Satellite Meteorological Center/national space weather monitoring and early warning center. Local meteorological data is obtained from www.tianqihoubao.com/lishi/zhengxiangbaiqi. Thanks to Lide Su, Jianxi Ren, Zhijun Chen, Linjie Chen, Zhichao Zhou, Cang Su, Suli Ma, Jun Cheng, Weijie Wang, Bingqing Pan, Fei Liu, Wei Wang, Jing Du, and Hongxia Nie, etc. from Mingantu Observing Station, Zhanwei Wu and Ming Zhang from the 54th institute of CETC, and Kaihua Deng and Wenqi Liu from the 16th institute of CETC, for their help in MST operation, observation and discussion.

References

- Benz, A. O., Guedel, M., Isliker, H., Miskowicz, S., & Stehling, W. 1991, *Sol. Phys.*, 133, 385
- Broten, N. W., & Medd, W. J. 1960, *ApJ*, 132, 279
- Findlay, J. W. 1966, *ARA&A*, 4, 77
- Fu, Q., Qin, Z., Ji, H., & Pei, L. 1995, *Sol. Phys.*, 160, 97
- Fu, Q., Ji, H., Qin, Z., et al. 2004, *Sol. Phys.*, 222, 167
- Geng, L. H., Tan, C. M., Dun, J. P., et al. 2018, *Astronomical Research & Technology*, 15, 380 (in Chinese)
- Gurnett, D. A. 1974, *J. Geophys. Res.*, 79, 4227
- Gurnett, D. A. 1975, *J. Geophys. Res.*, 80, 2751
- Ji, H.-R., Fu, Q.-J., Yan, Y.-H., et al. 2005, *ChJAA (Chin. J. Astron. Astrophys.)*, 5, 433
- Jiricka, K., Karlicky, M., Kepka, O., et al. 1993, *Sol. Phys.*, 147, 203
- Klein, K.-L., Matamoros, C. S., & Zucca, P. 2018, *Comptes Rendus Physique*, 19, 36
- Liu, S.-Q., Zhong, Q.-Z., Wen, J., & Dou, X.-K. 2010, *ChA&A*, 34, 305
- Matsuura, O. T., & Kaufmann, P. 1968, *Icarus*, 8, 193
- Messmer, P., Benz, A. O., & Monstein, C. 1999, *Sol. Phys.*, 187, 335
- Schonfeld, S. J., White, S. M., Henney, C. J., Arge, C. N., & McAteer, R. T. J. 2015, *ApJ*, 808, 29
- Tan, C., Yan, Y., Tan, B., et al. 2015, *ApJ*, 808, 61
- Tan, C., Yan, Y., Tan, B., & Xu, G. 2009, *Science in China: Physics, Mechanics and Astronomy*, 52, 1760
- Tanaka, H., Castelli, J. P., Covington, A. E., et al. 1973, *Sol. Phys.*, 29, 243
- Tsuchiya, A., & Nagame, K. 1965, *PASJ*, 17, 86
- Wen, J., Zhong, Q. Z., & Liu, S. Q. 2010, *Chin. J. Space Sci.*, 30, 198 (in Chinese)
- Yan, Y., Tan, C., Xu, L., et al. 2002, *Science in China A: Mathematics*, 45, 89
- Yan, Y., Zhang, J., Wang, W., et al. 2009, *Earth Moon and Planets*, 104, 97